

Variability in snow cover phenology in China from 1952 to 2010

Chang-Qing Ke^{1,2}, Xiu-Cang Li^{3,4}, Hongjie Xie⁵, Xun Liu^{1,2} and Cheng Kou^{1,2}

1. Jiangsu Provincial Key Laboratory of Geographic Information Science and Technology, Nanjing University, Nanjing, 210023, China.

2. Key Laboratory for Satellite Mapping Technology and Applications of State Administration of Surveying, Mapping and Geoinformation of China, Nanjing University, Nanjing, 210023, China.

3. National Climate Center, China Meteorological Administration, Beijing 100081, China.

4. Collaborative Innovation Center on Forecast and Evaluation of Meteorological Disasters, Faculty of Geography and Remote Sensing, Nanjing University of Information Science & Technology, Nanjing, 210044, China.

5. Department of Geological Sciences, University of Texas at San Antonio, Texas 78249, USA.

Correspondence to: C. Q. Ke (kecq@nju.edu.cn)

Tel: 0086-25-89685860

Fax: 0086-25-83592686

23 **Abstract** Daily snow observation data from 672 stations, particularly the 352 stations
24 with over ten annual mean snow cover days (SCD), during 1952–2010 in China, are
25 used in this study. We first examine spatiotemporal variations and trends of SCD, snow
26 cover onset date (SCOD), and snow cover end date (SCED). We then investigate SCD
27 relationships with number of days with temperature below 0°C (TBZD), mean air
28 temperature (MAT), and Arctic Oscillation (AO) index, the latter two being constrained
29 to the snow season of each snow year. The results indicate that years with positive SCD
30 anomaly for the entire country include 1955, 1957, 1964, and 2010, and years with
31 negative SCD anomaly include 1953, 1965, 1999, 2002, and 2009. The reduced TBZD
32 and increased MAT are the main reasons for the overall late SCOD and early SCED
33 since 1952, although it is not necessary for one station to experience both significantly
34 late SCOD and early SCED. This explains why only 15% of the stations show
35 significant shortening of SCD, while 75% of the stations show no significant change in
36 the SCD trends. This differs with the overall shortening of the snow period in the
37 Northern Hemisphere previously reported. Our analyses indicate that the SCD
38 distribution pattern and trends in China are very complex and are not controlled by any
39 single climate variable examined (i.e. TBZD, MAT, or AO), but a combination of
40 multiple variables. It is found that the AO has the maximum impact on the SCD
41 shortening trends in Shandong Peninsula, Changbai Mountains, and North Xinjiang,
42 while the combined TBZD and MAT have the maximum impact on the SCD shortening
43 trends in the Loess Plateau, Xiaoxinganling, and Sanjiang Plain.

44 **Keywords:** snow cover day; snow cover onset date; snow cover end date;

45 spatiotemporal variation; trend; days with temperature below 0°C; Arctic Oscillation

46

47 **Abbreviations:**

48 Snow Cover Day (SCD)

49 Snow Cover Onset Date (SCOD)

50 Snow Cover End Date (SCED)

51 Days with Temperature Below 0°C (TBZD)

52 Mean Air Temperature (MAT)

53 Arctic Oscillation (AO)

54

55 **1 Introduction**

56 Snow has a profound impact on the surficial and atmospheric thermal conditions,
57 and is very sensitive to climatic and environmental changes, because of its high
58 reflectivity, low thermal conductivity, and hydrological effects via snowmelt ([Barnett et
59 al., 1989](#); [Groisman et al., 1994](#)). The extent of snow cover in the Northern Hemisphere
60 decreased significantly over the past decades because of global warming ([Robinson and
61 Dewey 1990](#); [Brown and Robinson 2011](#)). Snow cover showed the largest decrease in
62 the spring, and the decrease rate increased for higher latitudes in response to larger
63 albedo feedback ([Déry and Brown, 2007](#)). In North America, snow depth in central
64 Canada showed the greatest decrease ([Dyer and Mote, 2006](#)), and snowpack in the

65 Rocky Mountains in the U.S. declined (Pederson et al., 2013). However, *in situ* data
66 showed a significant increase in snow accumulation in winter but a shorter snowmelt
67 season over Eurasia (Bulygina et al., 2009). Decreases in snow pack have also been
68 found for the European Alps in the last 20 years of the 20th century (Scherrer et al.,
69 2004), but a very long time series of snow pack suggests large decadal variability and
70 overall weak long-term trends only (Scherrer et al., 2013). Meteorological data
71 indicated that the snow cover over northwest China exhibited a weak upward trend in
72 depth (Qin et al., 2006), but the spatiotemporal variations were large (Ke et al., 2009;
73 Ma and Qin 2012). Simulation experiments using climate models indicated that, with
74 continuing global warming, the snow variation in China would show more differences
75 and uncertainties in space and time than ever before (Shi et al., 2011; Ji and Kang
76 2013). Spatiotemporal variations of snow cover are also manifested as snowstorms or
77 blizzards, particularly, excessive snowfall over a short time duration (Bolsenga and
78 Norton, 1992; Liang et al., 2008; Gao, 2009; Wang et al., 2013; Llasat et al., 2014).

79 Snow cover day (SCD) is an important index that represents the environmental
80 features of climate (Ye and Ellison 2003; Scherrer et al., 2004), and is directly related
81 to the radiation and heat balance of the Earth–atmosphere system. The SCD varies in
82 space and time and contributes to climate change over short time scales (Zhang, 2005),
83 especially in the Northern Hemisphere. Bulygina et al. (2009) investigated the linear
84 trends of SCD observed at 820 stations from 1966 to 2007, and indicated that the
85 duration of snow cover decreased in the northern regions of European Russia and in the
86 mountainous regions of southern Siberia, while it increased in Yakutia and the Far East.

87 Peng et al. (2013) analysed trends in the snow cover onset date (SCOD) and snow
88 cover end date (SCED) in relation to temperature over the past 27 years (1980–2006)
89 from over 636 meteorological stations in the Northern Hemisphere. They found that the
90 SCED remained stable over North America, whereas there was an early SCED over
91 Eurasia. Satellite snow data indicated that the average snow season duration over the
92 Northern Hemisphere decreased at a rate of 5.3 days per decade between 1972/73 and
93 2007/08 (Choi et al., 2010). Their results also showed that a major change in the trend
94 of snow duration occurred in the late 1980s, especially in the Western Europe, central
95 and East Asia, and mountainous regions in western United States.

96 There are large spatiotemporal differences in the SCD in China (Wang and Li,
97 2012). Analysis of 40 meteorological stations from 1971 to 2010 indicated that the
98 SCD had a significant decreasing trend in the western and south-eastern Tibetan
99 Plateau, with the largest decline observed in Nielamu, reaching 9.2 days per decade
100 (Tang et al., 2012). Data analysis also indicated that the SCD had a linear decreasing
101 trend at most stations in the Hetao region and its vicinity (Xi et al., 2009). However,
102 analysis of meteorological station data in Xinjiang showed that the SCD had a slight
103 increasing trend, occurring mainly in 1960–1980 (Wang et al., 2009b). Li et al. (2009)
104 analysed meteorological data from 80 stations in Heilongjiang Province, Northeast
105 China. Their results showed that the snow cover duration shortened, because of both the
106 late SCOD (by 1.9 days per decade) and early SCED (by 1.6 days per decade), which
107 took place mainly in the lower altitude plains.

108 The SCD is sensitive to local winter temperature and precipitation, latitude (Hantel

109 [et al., 2000](#); [Wang et al., 2009a](#); [Serquet et al., 2011](#); [Morán-Tejeda et al., 2013](#)), and
110 altitudinal gradient and terrain roughness ([Lehning et al., 2011](#); [Ke and Liu, 2014](#)).
111 Essentially, the SCD variation is mainly attributed to large-scale atmospheric
112 circulation or climatic forcing ([Beniston, 1997](#); [Scherrer and Appenzeller, 2006](#); [Ma
113 and Qin, 2012](#); [Birsan and Dumitrescu, 2014](#)), such as monsoons, El Niño/Southern
114 Oscillation (ENSO), North Atlantic Oscillation (NAO), and Arctic Oscillation (AO).
115 [Xu et al. \(2010\)](#) investigated the relationship between the SCD and monsoon index in
116 the Tibetan Plateau and indicated their great spatial differences. As an index of the
117 dominant pattern of non-seasonal sea-level pressure variations, the AO shows a large
118 impact on the winter weather patterns of the Northern Hemisphere ([Thompson and
119 Wallace, 1998](#); [Thompson et al., 2000](#); [Gong et al., 2001](#); [Wu and Wang, 2002](#); [Jeong
120 and Ho, 2005](#)). The inter-annual variation of winter extreme cold days in the northern
121 part of eastern China is closely linked to the AO ([Chen et al., 2013](#)). Certainly, the AO
122 plays an important role in the SCD variation. An increase in the SCD before 1990 and a
123 decrease after 1990 have been reported in the Tibetan Plateau, and snow duration has
124 positive correlations with the winter AO index ([You et al., 2011](#)), and a significant
125 correlation between the AO and snowfall over the Tibetan Plateau on inter-decadal
126 timescale was also reported by [Lü et al. \(2008\)](#).

127 The focus of this study is the variability in the snow cover phenology in China. A
128 longer time series of daily observations of snow cover is used for these spatial and
129 temporal analyses. We first characterize the spatial patterns of change in the SCD,
130 SCOD, and SCED in different regions of China; we then examine the sensitivity of

131 SCD to the number of days with temperature below 0°C (TBZD), the mean air
132 temperature (MAT), and the Arctic Oscillation (AO) index during the snow season
133 (between SCOD and SCED).

134 **2 Data and methods**

135 **2.1 Data**

136 We use daily snow cover and temperature data in China from 1 September 1951 to
137 31 August 2010, provided by the National Meteorological Information Centre of China
138 Meteorological Administration (CMA). According to the Specifications for Surface
139 Meteorological Observations ([China Meteorological Administration, 2003](#)), an SCD is
140 defined as a day when the snow cover in the area meets the following requirement: at
141 least half of the observation field is covered by snow. For any day with at least half of
142 the observation field covered by snow, snow depth is recorded as a rounded-up integer
143 if it is more than or equal to 0.5 cm (measured with a ruler), i.e. a normal SCD, whereas
144 the snow depth is denoted as 0 if it is less than 0.5 cm, i.e. a thin SCD. We define a
145 snow year as the period from 1 September of the previous year to 31 August of the
146 current year. For instance, September, October, and November 2009 are treated as the
147 autumn season of snow year 2010, December 2009 and January and February 2010 as
148 the winter season of snow year 2010, and March, April, and May 2010 as the spring
149 season of snow year 2010.

150 Station density is high in eastern China, where the observational data for most
151 stations are complete, with relatively long histories (as long as 59 years). Because of
152 topography and climate conditions, the discontinuous nature of snowfall is obvious in

153 western China, especially in the Tibetan Plateau, with patchy snow cover, and many
154 thin SCDs in these station records (Ke and Li, 1998). At the same time, in western
155 China, station density is low, and the observation history is relatively short, although
156 two of the three major snow regions are located in western China. If all stations with
157 short time series are eliminated, and thin SCDs are not taken into account, the spatial
158 representativeness of the dataset would be a problem. Therefore, a time series of at least
159 30 years is included in this study, including those thin SCDs. Totally, there are 722
160 stations in the original dataset.

161 Since station relocation and changes in the ambient environment could cause
162 inconsistencies in the recorded data, we implement strict quality controls (such as
163 inspection for logic, consistency, and uniformity) on the observational datasets in order
164 to reduce errors (Ren et al., 2005). The standard normal homogeneity test
165 (Alexandersson and Moberg, 1997) at the 95% confidence level is applied to the daily
166 SCD and temperature series data in order to identify possible breakpoints. Time series
167 gap filling is performed after all inhomogeneities are eliminated, using nearest
168 neighbour interpolation. After being processed as mentioned above, the 672 stations
169 with annual mean SCDs greater than 1.0 (day) are finally selected for subsequent
170 investigation (Fig. 1).

171 The observation period for each station is different, varying between 59 years
172 (1951/1952–2009/2010) and 30 years (1980/1981–2009/2010). Overall, 588 stations
173 have observation records between 50 and 59 years, 47 stations between 40 and 49 years,
174 and 37 stations between 30 and 39 years (Fig. 2). Most of the stations with observation

175 records of less than 50 years are located in remote or high elevation areas. All 672
176 stations are used to analyse the spatiotemporal distribution of SCD in China, while only
177 352 stations with more than ten annual mean SCDs are used to study the changes of
178 SCOD, SCED, and SCD relationships with TBZD, MAT, and the AO index.

179 The daily AO index constructed by projecting the daily (00Z) 1,000 mb height
180 anomalies poleward of 20°N from
181 http://www.cpc.ncep.noaa.gov/products/precip/CWlink/daily_ao_index/ao.shtml, is
182 used in this paper. A positive (negative) AO index corresponds to low (high) pressure
183 anomalies throughout the polar region and high (low) pressure anomalies across the
184 subtropical and mid-latitudes (Peings et al., 2013). We average the daily AO indexes
185 during the snow season of each station as the AO index of the year. A time series of AO
186 indexes from 1952 to 2010, for each of the 352 stations, is then constructed.

187 A digital elevation model (DEM) according to the Shuttle Radar Topographic
188 Mission (SRTM, <http://srtm.csi.cgiar.org>) of the National Aeronautics and Space
189 Administration (NASA) with a resolution of 90 m and the administration map of China
190 are used as the base map.

191 **2.2 Methods**

192 We apply Mann–Kendall (MK) test to analyse the trends of SCD, SCOD, and
193 SCED. The MK test is an effective tool to extract the trends of time series, and is
194 widely applied to the analysis of climate series (Marty, 2008). The MK test is
195 characterized as being more objective, since it is a non-parametric test. A positive
196 standardized MK statistic value indicates an upward or increasing trend, while a

197 negative value demonstrates a downward or decreasing trend. Confidence levels of
198 90% and 95% are taken as thresholds to classify the significance of positive and
199 negative trends of SCD, SCOD, and SCED.

200 At the same time, if SCD, SCOD, or SCED at one climate station has significant
201 MK trend (above 90%), their linear regression analyses are performed against time,
202 respectively. The slopes of the regressions represent the changing trends and are
203 expressed in days per decade. The statistical significance of the slope for each of the
204 linear regressions is assessed by the Student's t test (two-tailed test of the Student t
205 distribution), and only confidence levels above 90% are considered.

206 Correlation analysis is used to examine the SCD relationships with the TBZD,
207 MAT, and the AO index, and the Pearson product-moment correlation coefficients
208 (PPMCC) have been calculated. The PPMCC is a widely used estimator for describing
209 the spatial dependence of rainfall processes, and it indicates the strength of the linear
210 covariance between two variables ([Habib et al., 2001](#); [Ciach and Krajewski, 2006](#)). The
211 correlation coefficient can be defined as the covariance of the two variables (X , Y)
212 divided by the product of their standard deviations, giving a value between +1 and -1
213 inclusive, where 1 is total positive correlation, 0 is no correlation, and -1 is total
214 negative correlation. The statistical significance of the correlation coefficients is
215 calculated using the Student's t test, and only confidence levels above 90% are
216 considered in our analysis.

217 The spatial distribution of SCD, SCOD, and SCED, and their calculated results,
218 are spatially interpolated by applying the universal kriging method (assuming the data

219 is normally distributed). The universal kriging model is capable of simultaneously
220 treating multiple variables and their cross-covariance, and has been successfully applied
221 to spatial data interpolation (Kyriakidis and Goodchild, 2006). All mean errors are near
222 zero, all average standard errors are close to the corresponding root mean squared
223 errors, and all root mean squared standardized errors are close to 1 (Table 1). This fact
224 indicates that prediction errors are unbiased and valid, except for slightly overestimated
225 CV and slightly underestimated SCD in 2002. Overall, the interpolation results have
226 fewer errors and are acceptable.

227 **3 Results**

228 **3.1 Spatiotemporal variations of SCD**

229 **3.1.1 Spatial distribution of SCD**

230 The analysis of observations from 672 stations indicates that there are three major
231 stable snow regions with more than 60 annual mean SCDs: Northeast China, North
232 Xinjiang, and the Tibetan Plateau, with Northeast China being the largest of the three
233 (Fig. 3a). In the Daxingganling, Xiaoxingganling, and Changbai Mountains of
234 Northeast China, there are more than 90 annual mean SCDs, corresponding to a
235 relatively long snow season. The longest annual mean SCDs, 169 days, is at Arxan
236 Station (in the Daxinganling Mountains) in Inner Mongolia. In North Xinjiang, the
237 SCDs are relatively long in the Tianshan and Altun Mountains, followed by the Junggar
238 Basin. The annual mean SCDs in the Himalayas, Nyainqentanglha, Tanggula
239 Mountains, Bayan Har Mountains, Anemaqen Mountains, and Qilian Mountains of the
240 Tibetan Plateau are relatively long, although most of these areas have less than 60

241 annual SCDs. The Tibetan Plateau has a high elevation, a cold climate, and many
242 glaciers, but its mean SCD is not as large as that of the other two stable snow regions.

243 Areas with SCDs of 10–60 are called unstable snow areas with annual periodicity
244 (there is definitely snow every winter), including the peripheral parts of the three major
245 stable snow regions, and the Loess Plateau, Northeast Plain, North China Plain,
246 Shandong Peninsula, and areas in north of the Qinling-Huaihe line (along the Qinling
247 Mountains and Huaihe River to the east). Areas with SCDs of 1–10 are called unstable
248 snow areas without annual periodicity (the mountainous areas are excluded, not every
249 winter there is snow, especially in a warm winter), including the Tarim Basin, Qaidam
250 Basin, Badain Jaran Desert, the peripheral parts of Sichuan Basin, the northeast part of
251 the Yungui Plateau, and the middle and lower Yangtze River Plain. Areas with
252 occasional snow and mean annual SCD of less than 1.0 (day) are distributed north of
253 the Sichuan Basin and in the belt along Kunming, the Nanling Mountains, and Fuzhou
254 (approximate latitude of 25°N). Because of the latitude or local climate and terrain,
255 there is no snow in the Taklimakan Desert, Turpan Basin, the Yangtze River Valley in
256 the Sichuan Basin, the southern parts of Yunnan, Guangxi, Guangdong and Fujian, and
257 on the Hainan Island.

258 The spatial distribution pattern of SCD based on climate data with longer time
259 series is similar to previous studies (Li and Mi, 1983; Li, 1990; Liu et al., 2012; Wang
260 et al., 2009a; Wang and Li, 2012). The snow distribution is closely linked to latitude
261 and elevation, and is generally consistent with the climate zones (Lehning et al., 2011;
262 Ke and Liu, 2014). The higher the latitude, the lower the temperature and the more

263 SCDs there are. Therefore, there are relatively more SCDs in Northeast China and
264 North Xinjiang, and fewer SCDs to the south (Fig. 3a). In the Tibetan Plateau, located
265 in south-western China, the elevation is higher than eastern areas at the same latitude,
266 and the SCDs are greater than in eastern China (Tang et al., 2012). The amount of
267 precipitation also plays a critical role in determining the SCD (Hantel et al., 2000). In
268 the north-eastern coastal areas of China, which are affected considerably by the ocean,
269 there is much precipitation. In North Xinjiang, which has a typical continental (inland)
270 climate, the precipitation is less than in Northeast China, and there are more SCDs in
271 the north of Northeast China than in North Xinjiang (Dong et al., 2004; Wang et al.,
272 2009b). Moreover, the local topography has a relatively large impact on the SCD
273 (Lehning et al., 2011). The Tarim Basin is located inland, with relatively little
274 precipitation, thus snowfall there is extremely rare except for the surrounding
275 mountains (Li, 1993). The Sichuan Basin is surrounded by high mountains, therefore
276 situated in the precipitation shadow in winter, resulting in fewer SCDs (Li and Mi,
277 1983; Li, 1990).

278 The three major stable snow regions, Northeast China, North Xinjiang, and the
279 eastern Tibetan Plateau, have smaller coefficients of variation (CV) in the SCD (Fig.
280 3b). Nevertheless, the SCDs in arid or semi-arid areas, such as South Xinjiang, the
281 northern and south-western Tibetan Plateau, and central and western Inner Mongolia,
282 have large fluctuation because there is little precipitation during the cold seasons, and
283 certainly little snowfall and large CVs of SCD. In particular, the Taklimakan Desert in
284 the Tarim Basin is an extremely arid region, with only occasional snowfall. Therefore,

285 it has a very large range of SCD fluctuations. Additionally, the middle and lower
286 Yangtze River Plain also has large SCD fluctuations because of warm-temperate or
287 sub-tropic climate with short winter and little snowfall. Generally, the smaller the SCD,
288 the larger the CV (Wang et al., 2009a). This is consistent with other climate variables,
289 such as precipitation (Yang et al., 2015).

290 **3.1.2 Temporal variations of SCD**

291 Seasonal variation of SCD is primarily controlled by temperature and precipitation
292 (Hantel et al., 2000; Scherrer et al., 2004; Liu et al., 2012). In North Xinjiang and
293 Northeast China, snow is primarily concentrated in the winter (Fig. 4). In these regions,
294 the SCD exhibits a 'single-peak' distribution. In the Tibetan Plateau, however, the
295 seasonal variation of SCD is slightly different, i.e. more snow in the spring and autumn
296 combined than in the winter. The mean temperature and precipitation at Dangxiong
297 station (30°29' N, 91°06'E, 4200.0 m) in winter are -7.73° C and 7.92 mm, respectively,
298 and those at Qingshuihe station (33°48' N, 97°08'E, 4415.4 m) are -15.8° C and 16.3
299 mm, respectively. It is too cold and dry to produce enough snow in the Tibetan Plateau
300 (Hu and Liang, 2014)

301 The temporal variation of SCD shows very large differences from one year to
302 another. We define a year with a positive (negative) SCD anomaly in the following way:
303 for a given year, if 70% of the stations have a positive (negative) anomaly and 30% of
304 the stations have an SCD larger (smaller) than the mean \pm one standard deviation
305 (1SD), it is regarded as a year with a positive (negative) SCD anomaly. The years with
306 a positive SCD anomaly in China are 1955, 1957, 1964, and 2010 (Table 2). Moreover,

307 the stations with SCDs larger than the mean + 2SD account for 29% of all stations in
308 1955 and 1957, and these two years are considered as years with an extremely positive
309 SCD anomaly. In 1957, there was an almost nationwide positive SCD anomaly except
310 for North Xinjiang (Fig. 5a). This 1957 event had a great impact on agriculture, natural
311 ecology, and social-economic systems, and resulted in a tremendous disaster (Hao et al.,
312 2002). The year 2010 was also a year with a positive SCD anomaly in China. At the
313 same time, blizzards occurred in North America and Europe (including Spain) (Llasat
314 et al., 2014). Globally, an unusual cold weather pattern caused by high pressure (the
315 AO) brought cold, moist air from the north. Many parts of the Northern Hemisphere
316 experienced heavy snowfall and record-low temperatures, leading to, among other
317 things, a number of deaths, widespread transport disruption, and power failures
318 (http://en.wikipedia.org/wiki/Winter_of_2009–10_in_Europe, [http://en.wikipedia.org](http://en.wikipedia.org/wiki/February_9–10,_2010_North_American_blizzard)
319 [/wiki/February_9–10,_2010_North_American_blizzard](http://en.wikipedia.org/wiki/February_9–10,_2010_North_American_blizzard)). The blizzards across the
320 Texas and Oklahoma panhandles in 1957 (Bolsenga and Norton, 1992; Changnon and
321 Changnon, 2006) and across the east coast in 2010 were also recorded as the biggest
322 snowstorms of the United States from 1888 to the present
323 (<http://www.crh.noaa.gov/mkx/?n=biggestsnowstorms-us>).

324 Years with a negative SCD anomaly include 1953, 1965, 1999, 2002, and 2009
325 (Table 2). If there is too little snowfall in a specific year, a drought is possible. Drought
326 resulting from little snowfall in the cold season is a slow process and can sometimes
327 cause disasters. For example, East China displayed an apparent negative SCD anomaly
328 in 2002 (Fig. 5b), and had very little snowfall, leading to an extreme winter drought in

329 Northeast China, where snowfall is the primary form of winter precipitation (Fang et al.,
330 2014).

331 Because of different atmospheric circulation backgrounds, vapour sources, and
332 topographic conditions in different regions of China, there are great differences in the
333 SCD even in one year. For example, in 2008, there were more SCDs and longer snow
334 duration in the Yangtze River Basin, North China, and the Tianshan Mountains in
335 Xinjiang (Fig. 5c), especially in the Yangtze River Basin, where large snowfall is
336 normally not observed. However, four episodes of severe and persistent snow, extreme
337 low temperatures, and freezing weather occurred in early 2008, leading to a large-scale
338 catastrophe in this region where there were no mitigation measures for this type of a
339 disaster (Gao, 2009). As reported by the Ministry of Civil Affairs of China, the 2008
340 snow disaster killed 107 people and caused losses of US\$ 15.45 billion. Both the SCDs
341 and scale of economic damage broke records from the past five decades (Wang et al.,
342 2008). On the contrary, in the same year (2008), there was no snow disaster in North
343 Xinjiang, the Tibetan Plateau, and Pan-Bohai Bay region. Moreover, Northeast China
344 had an apparent negative SCD anomaly (Fig. 5c).

345 There are great differences in the temporal variations of SCD even in the three
346 major stable snow regions. If we redefine a year with a positive (negative) SCD
347 anomaly, using the much higher standard that 80% of stations should have a positive
348 (negative) anomaly and 40% of stations should have an SCD larger (smaller) than the
349 mean ± 1 SD. It is found that 1957, 1973, and 2010 are years with a positive SCD
350 anomaly in Northeast China, while 1959, 1963, 1967, 1998, 2002, and 2008 are years

351 with a negative SCD anomaly there (Table 3, Fig. 5a–c). Years with a positive SCD
352 anomaly in North Xinjiang include 1959, 1960, 1977, 1980, 1988, 1994, and 2010, and
353 years with a negative SCD anomaly include 1974, 1995, and 2008 (Table 3, Fig. 5c).
354 North Xinjiang is one of the regions prone to catastrophe, where frequent heavy
355 snowfall greatly affects the development of animal husbandry (Hao et al., 2002).

356 Years with a positive SCD anomaly in the Tibetan Plateau include 1983 and 1990,
357 whereas years with a negative SCD anomaly include 1965, 1969, and 2010 (Table 3).
358 The climate in the Tibetan Plateau is affected by the Indian monsoon from the south,
359 westerlies from the west, and the East Asian monsoon from the east (Yao et al., 2012).
360 Therefore, there is a regional difference in the SCD within the Tibetan Plateau, and
361 even a difference in the spatiotemporal distribution of snow disasters (Wang et al.,
362 2013). Our results differ from the conclusions drawn by Dong et al. (2001), as they
363 only used data from 26 stations, covering only a short period (1967–1996).

364 **3.1.3 SCD trends**

365 Changing trends of annual SCDs are examined, as shown in Figure 6, and
366 summarized in Table 4. Among the 352 stations, there are 54 stations (15%) with a
367 significant negative trend, and 35 stations (10%) with a significant positive trend (both
368 at the 90% level), while 75% of stations show no significant trends. The SCD exhibits a
369 significant downward trend in the Shandong Peninsula, and insignificant downward
370 trends in the North China Plain, the Loess Plateau, the Xiaoxingganling, the Changbai
371 Mountains, North Xinjiang, Northeast Qinghai, and the south-western Tibetan Plateau
372 (Fig. 6a). Some station records indicate a decreasing rate of 1.3–7.2 days per decade.

373 For example, the SCD decreased by 40 days from 1955 to 2010 at the Kuandian station
374 in Northeast China, 30 days from 1954 to 2010 at the Hongliuhe station in Xinjiang,
375 and 15 days from 1958 to 2010 at the Gangcha station on the Tibetan Plateau (Fig.
376 7a–c).

377 The SCDs in the Bayan Har Mountains, the Anemaqen Mountains, the Inner
378 Mongolia Plateau, and Daxingganling, exhibit a significant upward trend (Fig. 6a). For
379 example, at the Shiqu station on the eastern border of the Tibetan Plateau, the SCD
380 increased 26 days from 1960 to 2010 (Fig. 7d). The coexistence of negative and
381 positive trends in the SCD change was also reported by Bulygina et al. (2009) and
382 Wang and Li (2012).

383 **3.2 Spatiotemporal variations of SCOD**

384 **3.2.1 SCOD variations**

385 The SCOD is closely related to both latitude and elevation (Fig. 8a). For example,
386 snowfall begins in September on the Tibetan Plateau, in early or middle October on the
387 Daxingganling, and in middle or late October on the Altai Mountains of Xinjiang. The
388 SCOD also varies from one year to another (Table 2). Using the definition of a year
389 with a positive (negative) SCD anomaly, as introduced before (i.e. 70% stations with
390 positive (negative) SCOD anomaly and 30% stations with SCOD larger (smaller) than
391 the mean \pm 1SD), we consider a given year as a late (early) SCOD year. Only two
392 years, 1996 and 2006, can be considered as late SCOD years on a large scale (Table 2),
393 especially in 2006, in East China and the Tibetan Plateau (Fig.6d), while not any single
394 year can be considered as an early SCOD year.

395 **3.2.2 SCOD trends**

396 There are 136 stations (39%) with a significant trend of late SCOD, and 23
397 stations (7%) with a significant trend of early SCOD (both at the 90% level), while
398 54% of the stations show no significant trends (Table 4). The SCOD in Northeast China,
399 the central and eastern Tibetan Plateau, the upper reach of the Yellow River, North
400 Gansu, and North Xinjiang exhibits a significant trend towards late SCOD (Fig. 6b).
401 These significantly late trends dominate the major snow areas of China. In particular,
402 the late SCOD in Northeast China is consistent with a previous study (Li et al., 2009).
403 The SCOD in the Pan-Bohai Bay region and the Tianshan Mountains exhibits a trend
404 towards early SCOD. However, this trend is only significant in the Liaoxi corridor and
405 the Tianshan Mountains. For example, the SCOD at the Pingliang station in Gansu
406 Province shows a late rate of 5.2 days per decade from 1952 to 2010, but the SCOD at
407 the Weichang station in Hebei Province shows an early rate of 5.2 days per decade
408 from 1952 to 2010 (Fig. 7e–f).

409 **3.3 Spatiotemporal variations of SCED**

410 **3.3.1 SCED variations**

411 The pattern of SCED is similar to that of SCOD (Fig. 8b), i.e. places with early
412 snowfall normally show late snowmelt, while places with late snowfall normally show
413 early snowmelt. Like the SCOD, temporal variations of SCED are large (Table 2).
414 Using the same standard for defining the SCOD anomaly, we judge a given year as a
415 late (early) SCED year. It is evident that 1957 was a typical year whose SCED was late,
416 which was also the reason for the great SCDs (Table 2, Fig. 5e). The SCEDs in 1997

417 and 2004 were very early. For example, in 1997, the SCED was early for almost all of
418 China except for the Tibetan Plateau, western Tianshan, and western Liaoning (Fig. 5f).
419 In general, the early SCED is dominant and more evident than the late SCED (Table 2).

420 **3.3.2 SCED trends**

421 For the SCED, there are 138 stations (39%) with a significantly early trend (at the
422 90% level), while 60% of stations show no significant trends (Table 4). Major snow
423 areas in China all show early SCED, significant for Northeast China and the Tibetan
424 Plateau (Fig. 6c). The tendency of late SCED is limited, with only two stations showing
425 a significant trend. For example, the SCED at the Jixi station in Northeast China shows
426 an early rate of 4.4 days per decade from 1952 to 2010, while the SCED at the
427 Maerkang station in Sichuan Province shows a late rate of 4.2 days per decade from
428 1954 to 2010 (Fig. 7g–h).

429 **4 Discussion**

430 In the context of global warming, 136 stations (39%) show significantly late
431 SCOD, and 138 stations (39%) show significantly early SCED, all at the 90%
432 confidence level. It is not necessary for one station to show both significantly late
433 SCOD and early SCED. This explains why only 15% of stations show a significantly
434 negative SCD trend, while 75% of stations show no significant change in the SCD
435 trends. The latter is inconsistent with the overall shortening of the snow period in the
436 Northern Hemisphere reported by Choi et al. (2010). One reason could be the different
437 time periods used in the two studies, 1972–2007 in Choi et al. (2010) as compared with
438 1952–2010 in this study. Below, we discuss the possible connections between the

439 spatiotemporal variations of snow cover and the warming climate and changing AO.

440 **4.1 Relationship with TBZD**

441 The number of days with temperature below 0°C (TBZD) plays an important role
442 in the SCD. There are 330 stations (94% of all stations) showing positive correlations
443 between TBZD and SCD, with 193 of them (55%) having significantly positive
444 correlations (Table 4, Fig. 6d). For example, there is a significantly positive correlation
445 between SCD and TBZD at the Chengshantou station (Fig. 9a). Therefore, generally
446 speaking, the smaller the TBZD, the shorter the SCD.

447 For the SCOD, there are 287 stations with negative correlations with TBZD,
448 accounting for 82% of 352 stations, whereas only 63 stations (18%) show positive
449 correlations (Table 4). This means that for smaller TBZD, the SCOD is later. For the
450 SCED, there are 318 stations with positive correlations, accounting for 90% of 352
451 stations, whereas only 34 stations (10%) have negative correlations. This means that for
452 smaller TBZD, the SCED is earlier.

453 Very similar results are found for MAT (Table 4, Fig. 6e), and Fig. 9b shows an
454 example (the Baicheng station).

455 **4.2 Relationship with AO**

456 Although the AO index showed a strong positive trend in the past decades
457 (Thompson et al., 2000), its impact on the SCD in China is spatially distinctive.
458 Positive correlations (47% of 352 stations) are found in central China, i.e. the eastern
459 Tibetan Plateau, the upper reach of the Yangtze River, and the upper and middle
460 reaches of the Yellow River (Table 4, Fig. 6f), and Fig. 9c shows an example (the

461 Huajialing station). Negative correlations (53% of 352 stations) exist in North Xinjiang,
462 the Changbaishan Mountain and the coasts of the Liaoning and Shandong Peninsula,
463 and Fig. 9d shows an example (the Tonghua station).

464 **5 Conclusion**

465 This study examines the snow cover change based on 672 stations in 1952–2010 in
466 China. Specifically, the 352 stations with more than ten annual mean SCDs are used to
467 study the changing trends of SCD, SCOD, and SCED, and SCD relationships with
468 TBZD, MAT, and AO index during snow seasons. Some important results are
469 summarized below.

470 Northeast China, North Xinjiang, and the Tibetan Plateau are the three major snow
471 regions, with Northeast China being the largest. In North Xinjiang and in central and
472 north-eastern China, the SCDs are concentrated in the winter season. On the Tibetan
473 Plateau, however, snowfall is more frequent in the spring and fall. The overall
474 inter-annual variability of SCD is large in China. The years with a positive SCD
475 anomaly in China include 1955, 1957, 1964, and 2010, while the years with a negative
476 SCD anomaly are 1953, 1965, 1999, 2002, and 2009. Only 15% of stations show a
477 significantly negative SCD trend, while 75% of stations show no significant SCD
478 trends. This differs from the overall shortening of the snow period in the Northern
479 Hemisphere previously reported. One reason could be the different time periods used in
480 the two studies, 1972–2007 in the work of Choi et al. (2010) compared with 1952–2010
481 in this study. Our analyses indicate that the SCD distribution pattern and trends in
482 China are very complex and are not controlled by any single climate variable examined

483 (i.e. TBZD, MAT, or AO), but a combination of multiple variables. However, it seems
484 that the AO index has the most impact on the SCD shortening trends in the Shandong
485 Peninsula, Changbai Mountains, and North Xinjiang; the combination of smaller TBZD
486 and increasing MAT has the largest impact on the SCD shortening trends on the Loess
487 Plateau, Xiaoxingganling, and the Sanjiang Plain.

488 It is found that significantly late SCOD occurs in Northeast China, the central and
489 eastern Tibetan Plateau, the upper reach of the Yellow River, North Gansu, and North
490 Xinjiang; significantly early SCED occurs in Northeast China and the Tibetan Plateau.
491 Both the SCOD and SCED are closely related to the TBZD and MAT, and are mostly
492 controlled by local latitude and elevation. Owing to global warming since 1950s, the
493 reduced TBZD and increased MAT are the main reasons for overall late SCOD and
494 early SCED, although it is not necessary for one station to experience both significantly
495 late SCOD and early SCED. This explains why only 15% of stations show significantly
496 negative SCD trends, while 75% of stations show no significant SCD trends.

497 Long-duration, consistent records of snow are rare in China because of many
498 challenges associated with taking accurate and representative measurements, especially
499 in western China. The station density and metric choice also vary with time and locality,
500 therefore, more accurate and reliable observation data are needed to further analyse the
501 spatiotemporal distribution and features of snow cover phenology. Atmospheric
502 circulation causes variability in the snow cover phenology, and this effect also requires
503 deeper investigation.

504

505 **Acknowledgments**

506 This work is financially supported by the Program for National Nature Science
507 Foundation of China (No. 41371391), and the Program for the Specialized Research
508 Fund for the Doctoral Program of Higher Education of China (No. 20120091110017).

509 This work is also partially supported by Collaborative Innovation Center of Novel
510 Software Technology and Industrialization. We would like to thank the National
511 Climate Center of China (NCC) in Beijing for providing valuable climate datasets. We
512 thank the three anonymous reviewers and the editor for valuable comments and
513 suggestions that greatly improved the quality of this paper.

514 **References**

515 An, D., Li, D., Yuan, Y. and Hui, Y.: Contrast between snow cover data of different
516 definitions, *J. Glaciol. Geocrol.*, 31(6), 1019-1027, 2009.

517 Alexandersson, H. and Moberg, A.: Homogenization of Swedish temperature data Part
518 1: homogeneity test for linear trends, *Int. J. Climatol.*, 17, 25-34, 1997.

519 Barnett, T. P., Dumenil, L. and Latif, M.: The effect of Eurasian snow cover on regional
520 and global climate variations, *J. Atmos. Sci.*, 46, 661-685, 1989.

521 Beniston, M: Variations of snow depth and duration in the Swiss Alps over the last 50
522 years: Links to changes in large-scale climatic forcings, *Clim. Change*, 36, 281-300,
523 1997.

524 Birsan, M. V. and Dumitrescu, A.: Snow variability in Romania in connection to
525 large-scale atmospheric circulation, *Int. J. Climatol.*, 34, 134-144, 2014.

526 Bolsenga, S. J., and Norton, D. C.: Maximum snowfall at long-term stations in the
527 U.S./Canadian Great Lakes, *Nat. Hazards*, 5, 221-232, 1992.

528 Brown, R. D. and Robinson, D. A.: Northern Hemisphere spring snow cover variability
529 and change over 1922-2010 including an assessment of uncertainty, *The Cryosphere*,
530 5, 219-229, 2011.

531 Bulygina, O. N., Razuvaev, V. N. and Korshunova, N. N.: Changes in snow cover over
532 Northern Eurasia in the last few decades, *Environ. Res. Lett.*, 4, 045026, 2009.

533 Changnon, S. A. and Changnon, D.: A spatial and temporal analysis of damaging
534 snowstorms in the United States, *Nat. Hazards*, 37, 373-389, 2006.

535 Chen, S., Chen, W. and Wei, K.: Recent trends in winter temperature extremes in
536 eastern China and their relationship with the Arctic Oscillation and ENSO, *Adv.*
537 *Atmos. Sci.*, 30, 1712-1724, 2013.

538 China Meteorological Administration: Specifications for Surface Meteorological
539 Observations, Beijing, China Meteorological Press, 1-62, 2003.

540 Choi, G., Robinson, D. A. and Kang, S.: Changing Northern Hemisphere snow seasons,
541 *J. Climate*, 23, 5305-5310, 2010.

542 Ciach, G. J. and Krajewski, W. F.: Analysis and modeling of spatial correlation
543 structure in small-scale rainfall in Central Oklahoma, *Adv. Water Resour.*, 29(10),
544 1450–1463, 2006.

545 Déry, S. J. and Brown, R. D.: Recent Northern Hemisphere snow cover extent trends
546 and implications for the snow-albedo feedback, *Geophys. Res. Lett.*, 34, L22504,
547 2007.

548 Dong, A., Guo, H., Wang, L. and Liang, T.: A CEOF analysis on variation about yearly
549 snow days in Northern Xinjiang in recent 40 years, *Plateau Meteorol.*, 23, 936-940,
550 2004.

551 Dong, W., Wei, Z. and Fan, J.: Climatic character analysis of snow disasters in east
552 Qinghai-Xizang Plateau livestock farm, *Plateau Meteorol.*, 20, 402-406, 2001.

553 Dyer, J. L. and Mote, T. L.: Spatial variability and trends in observed snow depth over
554 North America, *Geophys. Res. Lett.*, 33, L16503, 2006

555 Fang, S., Qi, Y., Han, G., Zhou, G. and Cammarano, D.: Meteorological drought trend
556 in winter and spring from 1961 to 2010 and its possible impacts on wheat in wheat
557 planting area of China, *Sci. Agricul. Sin.*, 47, 1754-1763, 2014

558 Gao, H.: China's snow disaster in 2008, who is the principal player? *Int. J. Climatol.*, 29,
559 2191-2196, 2009.

560 Gong, D. Y., Wang, S. W. and Zhu, J. H.: East Asian winter monsoon and Arctic
561 oscillation, *Geophys. Res. Lett.*, 28, 2073-2076, 2001.

562 Groisman, P. Y., Karl, T. R. and Knight, R. W.: Observed impact of snow cover on the
563 heat-balance and the rise of continental spring temperatures, *Science*, 263, 198-200,
564 1994.

565 Habib, E., Krajewski, W. F. and Ciach, G. J.: Estimation of rainfall interstation
566 correlation, *J. Hydrometeorol.*, 2(6), 621–629, 2001.

567 Hantel, M., Ehrendorfer, M. and Haslinger, A.: Climate sensitivity of snow cover
568 duration in Austria, *Int. J. Climatol.*, 20, 615-640, 2000.

569 Hao, L., Wang, J., Man, S. and Yang, C.: Spatio-temporal change of snow disaster and
570 analysis of vulnerability of animal husbandry in China, *J. Nat. Disaster*, 11, 42-48,
571 2002.

572 He, L. and Li, D.: Classification of snow cover days and comparing with satellite
573 remote sensing data in west China, *J. Glaciol. Geocrol.*, 33(2), 237-245, 2011.

574 Hu, H. and Liang, L.: Temporal and spatial variations of snowfall in the east of
575 Qinghai-Tibet Plateau in the last 50 years, *Acta Geogr. Sin.*, 69, 1002-1012, 2014.

576 Jeong, J. H. and Ho, C. H.: Changes in occurrence of cold surges over East Asia in
577 association with Arctic oscillation, *Geophys. Res. Lett.*, 32, L14704, 2005.

578 Ji, Z. and Kang, S.: Projection of snow cover changes over China under RCP scenarios
579 *Clim. Dyn.*, 41, 589-600, 2013.

580 Ke, C. Q. and Li, P. J.: Spatial and temporal characteristics of snow cover over the
581 Tibetan plateau, *Acta Geogr. Sin.*, 53, 209-215, 1998.

582 Ke, C. Q. and Liu, X.: MODIS-observed spatial and temporal variation in snow cover in
583 Xinjiang, China, *Clim. Res.*, 59, 15-26, 2014.

584 Ke, C. Q., Yu, T., Yu, K., Tang, G. D. and King, L.: Snowfall trends and variability in
585 Qinghai, China, *Theor. Appl. Climatol.*, 98, 251-258, 2009.

586 Kyriakidis, P. C. and Goodchild, M. F.: On the prediction error variance of three
587 common spatial interpolation schemes, *Int. J. Geogr. Info. Science*, 20(8), 823-855,
588 2006.

589 Lehning, M., Grünewald, T. and Schirmer, M.: Mountain snow distribution governed by
590 an altitudinal gradient and terrain roughness, *Geophys. Res. Lett.*, 38, L19504, 2011.

591 Li, D., Liu, Y., Yu, H. and Li, Y.: Spatial-temporal variation of the snow cover in
592 Heilongjiang Province in 1951-2006, *J. Glaciol. Geocrol.*, 31, 1011-1018, 2009.

593 Li, J. and Wang, J.: A modified zonal index and its physical sense, *Geophys. Res. Lett.*,
594 30, 1632, 2003.

595 Li, L. Y. and Ke, C. Q.: Analysis of spatiotemporal snow cover variations in Northeast
596 China based on moderate-resolution-imaging spectroradiometer data, *J. Appl.*
597 *Remote Sens.*, 8, 084695, doi: 10.1117/1.JRS.8.084695. 2014.

598 Li, P. J.: Dynamic characteristic of snow cover in western China, *Acta Meteorol. Sin.*,
599 48, 505-515, 1993.

600 Li, P. J.: A preliminary study of snow mass variations over past 30 years in China, *Acta*
601 *Geogr. Sin.*, 48, 433-437, 1990.

602 Li, P. J. and Mi, D.: Distribution of snow cover in China, *J. Glaciol. Geocrol.*, 5, 9-18,
603 1983.

604 Liang, T. G., Huang, X. D., Wu, C. X., Liu, X. Y., Li, W. L., Guo, Z. G. and Ren, J. Z.:
605 An application of MODIS data to snow cover monitoring in a pastoral area: A case
606 study in Northern Xinjiang, China, *Remote Sens. Environ.*, 112, 1514-1526, 2008.

607 Liu, Y., Ren, G. and Yu, H.: Climatology of Snow in China, *Sci. Geogr. Sin.*, 32,
608 1176-1185, 2012.

609 Llasat, M. C., Turco, M., Quintana-Seguí, P. and Llasat-Botija, M.: The snow storm of
610 8 March 2010 in Catalonia (Spain): a paradigmatic wet-snow event with a high
611 societal impact, *Nat. Hazards Earth Syst. Sci.*, 14, 427-441, 2014.

612 Lü, J. M., Ju, J. H., Kim, S. J., Ren, J. Z. and Zhu, Y. X.: Arctic Oscillation and the
613 autumn/winter snow depth over the Tibetan Plateau, *J. Geophys. Res.*, 113, D14117,
614 2008.

615 Ma, L. and Qin, D.: Temporal-spatial characteristics of observed key parameters of
616 snow cover in China during 1957-2009, *Sci. Cold Arid Reg.*, 4, 384-393, 2012.

617 Marty, C.: Regime shift of snow days in Switzerland, *Geophys. Res. Lett.*, 35, L12501,
618 2008.

619 Morán-Tejeda, E., López-Moreno, J. I. and Beniston, M.: The changing roles of
620 temperature and precipitation on snowpack variability in Switzerland as a function of
621 altitude, *Geophys. Res. Lett.*, 40, 2131-2136, 2013.

622 Pederson, G. T., Betancourt, J. L. and Gregory, J. M.: Regional patterns and proximal
623 causes of the recent snowpack decline in the Rocky Mountains, U.S., *Geophys. Res.*
624 *Lett.*, 40, 1811-1816, 2013.

625 Peings, Y., Brun, B., Mauvais, V. and Douville, H.: How stationary is the relationship
626 between Siberian snow and Arctic Oscillation over the 20th century, *Geophys. Res.*
627 *Lett.*, 40, 183-188, 2013.

628 Peng, S., Piao, S., Ciais, P., Fang, J. and Wang, X.: Change in winter snow depth and its
629 impacts on vegetation in China, *Glob. Change Biol.*, 16, 3004-3013, 2010.

630 Peng, S., Piao, S., Ciais, P., Friedlingstein, P., Zhou, L. and Wang, T.: Change in snow
631 phenology and its potential feedback to temperature in the Northern Hemisphere over
632 the last three decades, *Environ. Res. Lett.*, 8, 014008, 2013.

633 Qin, D., Liu, S. and Li, P.: Snow cover distribution, variability, and response to climate
634 change in western China, *J. Climate*, 19, 1820-1833, 2006.

635 Ren, G. Y., Guo, J., Xu, M. Z., Chu, Z. Y., Zhang, L., Zou, X. K., Li, Q. X. and Liu, X.
636 N.: Climate changes of China's mainland over the past half century, *Acta. Meteorol.*
637 *Sin.*, 63, 942-956, 2005.

638 Robinson, D. A. and Dewey, K. F.: Recent secular variations in the extent of northern
639 hemisphere snow cover, *Geophys. Res. Lett.*, 17, 1557-1560, 1990.

640 Scherrer, S. C., Appenzeller, C. and Laternser, M.: Trends in Swiss Alpine snow days:
641 The role of local- and large-scale climate variability, *Geophys. Res. Lett.*, 31, L13215,
642 2004.

643 Scherrer, S. C. and Appenzeller, C.: Swiss Alpine snow pack variability: major patterns
644 and links to local climate and large-scale flow, *Clim. Res.*, 32(3), 187-199, 2006.

645 Scherrer, S. C., Wüthrich, C., Croci-Maspoli, M., Weingartner, R. and Appenzeller, C.:
646 Snow variability in the Swiss Alps 1864-2009, *Int. J. Clim.*, 33(15), 3162 – 3173,
647 2013, doi: 10.1002/joc.3653.

648 Serquet, G., Marty, C., Dulex, J-P. and Rebetez, M.: Seasonal trends and temperature
649 dependence of the snowfall/precipitation-day ratio in Switzerland, *Geophys. Res. Lett.*, 38, L07703, 2011.

651 Shi, Y., Gao, X., Wu, J. and Giorgi, F.: Changes in snow cover over China in the 21st
652 century as simulated by a high resolution regional climate model, *Environ. Res. Lett.*,
653 6, 045401, 2011.

654 Tang, X., Yan, X., Ni, M. and Lu, Y.: Changes of the snow cover days on Tibet Plateau
655 in last 40 years, *Acta. Geogr. Sin.*, 67, 951-959, 2012.

656 Thompson, D. W. J. and Wallace, J. M.: The Arctic oscillation signature in the
657 wintertime geopotential height and temperature fields, *Geophys. Res. Lett.*, 25,
658 1297-1300, 1998.

659 Thompson, D. W. J., Wallace, J. M. and Hegerl, G. C.: Annular modes in the
660 extratropical circulation, part II: Trends, *J. Climate*, 13, 1018-1036, 2000.

661 Wang, C. and Li, D.: Spatial-temporal variations of the snow cover days and the
662 maximum depth of snow cover in China during recent 50 years, *J. Glaciol. Geocrol.*,
663 34, 247-256, 2012.

664 Wang, C., Wang, Z. and Cui, Y.: Snow cover of China during the last 40 years: Spatial
665 distribution and interannual variation, *J. Glaciol. Geocrol.*, 31, 301-310, 2009a.

666 Wang, J. and Hao, X.: Responses of snowmelt runoff to climatic change in an inland
667 river basin, Northwestern China, over the past 50 years, *Hydrol. Earth Syst. Sci.*, 14,
668 1979-1987, 2010.

669 Wang, L. et al.: Characteristics of the extreme low-temperature, heavy snowstorm and
670 freezing disasters in January 2008 in China, *Meteorol. Mon.*, 34, 95-100, 2008.

671 Wang, Q., Zhang, C., Liu, J. and Liu, W.: The changing tendency on the depth and days
672 of snow cover in Northern Xinjiang, *Adv. Clim. Change Res.*, 5, 39-43, 2009b.

673 Wang, W., Liang, T., Huang, X., Feng, Q., Xie, H., Liu, X., Chen, M. and Wang, X.:
674 Early warning of snow-caused disasters in pastoral areas on the Tibetan Plateau, *Nat.*
675 *Hazards Earth Syst. Sci.*, 13, 1411-1425, 2013.

676 Wu, B. Y. and Wang, J.: Winter Arctic oscillation, Siberian high and East Asian winter
677 monsoon, *Geophys. Res. Lett.*, 29, 1897, 2002.

678 Xi, Y., Li, D. and Wang, W.: Study of the temporal-spatial characteristics of snow
679 covers days in Hetao and its vicinity, *J. Glaciol. Geocrol.*, 31, 446-456, 2009.

680 Xu, L., Li, D. and Hu, Z.: Relationship between the snow cover day and monsoon index
681 in Tibetan Plateau, *Plateau Meteorol.*, 29, 1093-1101, 2010.

682 Yang, H., Yang, D., Hu, Q. and Lv, H.: Spatial variability of the trends in climatic
683 variables across China during 1961-2010, *Theor. Appl. Climatol.*, 2015 (in press).

684 Yao, T. et al.: Different glacier status with atmospheric circulations in Tibetan Plateau
685 and surroundings, *Nature Clim. Change*, 2, 663-667, 2012.

686 Ye, H. and Ellison, M.: Changes in transitional snowfall season length in northern
687 Eurasia, *Geophys. Res. Lett.*, 30, 1252, 2003.

688 You, Q., Kang, S., Ren, G., Fraedrich, K., Pepin, N., Yan, Y. and Ma, L.: Observed
689 changes in snow depth and number of snow days in the eastern and central Tibetan
690 Plateau, *Clim. Res.*, 46, 171-183, 2011.

691 Zhang, T.: Influence of the seasonal snow cover on the ground thermal regime: An
692 overview, *Rev. Geophys.*, 43, 1-23, 2005.

693

694

695 **Table Captions**

696 **Table 1.** Prediction errors of cross validation for the spatial interpolation with the
697 universal kriging method.

Item (Figure)	Mean error	Average standard error	Root mean squared error	Root mean squared standardized error
SCD (Fig.3a)	-0.0078	9.3710	10.3351	1.1729
CV (Fig.3b)	0.0027	70.9203	56.7797	0.8236
SCD in 1957 (Fig.5a)	-0.0001	10.1066	11.6712	1.1430
SCD in 2002 (Fig.5b)	0.0170	5.7430	7.9122	1.2862
SCD in 2008 (Fig.5c)	0.0008	6.8352	7.3988	1.0627
SCED in 1957 (Fig.5d)	0.0050	14.7432	14.8384	1.0112
SCED in 1997 (Fig.5e)	0.0026	16.9098	19.5960	1.1420
SCOD in 2006 (Fig.5f)	-0.0035	15.4075	16.2315	1.0396
SCOD (Fig.8a)	0.0037	13.8313	15.3312	1.1001
SCED (Fig.8b)	-0.0038	17.1397	19.9136	1.1376

698

699

700

701

702

703

704

705

706 **Table 2.** Percentage (%) of stations with anomalies (P for positive and N for negative)

707 of snow cover day (SCD), snow cover onset date (SCOD), and snow cover end date

708 (SCED). Percentage (%) of stations with anomalies of SCD, SCOD, and SCED larger

709 (smaller) than the mean +/- one or two standard deviations (1SD or 2SD), with the bold

710 number denoting years with a positive (negative) SCD anomaly, and late (early) years

711 for SCOD or SCED in China. All the percentages are calculated based on 672 stations.

712

Year	SCD						SCOD						SCED					
	P	1SD	2SD	-2SD	-1SD	N	P	1SD	2SD	-2SD	-1SD	N	P	1SD	2SD	-2SD	-1SD	N
1952	33	5	0	12	31	67	67	39	21	2	12	33	57	17	2	11	16	43
1953	30	6	0	3	34	70	40	8	2	2	18	60	39	9	1	9	17	61
1954	59	29	11	0	8	41	36	8	4	1	17	64	57	12	0	0	9	43
1955	80	48	29	1	5	20	35	8	3	1	24	65	78	21	2	1	5	22
1956	48	11	0	0	4	52	70	20	2	0	8	30	62	23	1	2	12	38
1957	85	64	29	0	3	15	25	5	1	0	14	75	85	35	5	1	4	15
1958	45	15	4	0	14	55	46	17	0	0	19	54	51	16	3	3	17	49
1959	27	6	1	4	23	73	55	27	9	1	17	45	57	22	3	1	5	43
1960	37	12	2	0	15	63	47	10	2	2	13	53	60	25	5	4	17	40
1961	34	7	1	1	19	66	24	9	2	1	28	76	29	6	1	9	28	71
1962	40	10	3	0	10	60	43	13	4	2	10	57	60	18	3	0	11	40
1963	24	5	1	1	25	76	33	13	5	1	26	67	52	14	0	8	16	48
1964	77	39	11	0	1	23	30	3	1	4	23	70	66	17	1	0	5	34
1965	25	8	0	1	33	75	56	18	5	1	9	44	56	14	2	3	16	44
1966	27	7	1	0	12	73	46	20	5	0	12	54	69	12	1	1	4	31
1967	32	7	1	3	23	68	39	10	3	1	14	61	44	4	0	3	11	56
1968	59	28	11	3	8	41	37	9	1	0	13	63	33	13	0	4	27	67
1969	45	21	8	4	21	55	45	13	1	3	19	55	68	21	1	1	7	32
1970	44	14	1	2	10	56	37	10	3	2	26	63	64	18	3	0	6	36
1971	52	12	1	1	11	48	38	14	4	1	17	63	54	8	1	1	9	46
1972	56	24	11	0	7	44	38	10	3	1	20	62	45	16	4	1	9	55
1973	49	19	2	1	7	51	37	10	1	1	22	63	44	9	1	1	8	56
1974	34	9	0	3	23	66	55	30	6	1	10	45	54	12	1	1	9	46
1975	40	9	3	1	14	60	26	7	2	1	21	74	42	14	3	3	17	58
1976	35	11	3	1	22	65	58	24	11	0	5	42	76	29	5	1	3	24
1977	45	20	3	0	9	55	29	5	1	0	24	71	55	14	3	2	12	45
1978	58	21	8	0	2	42	45	13	2	2	12	55	53	10	1	0	8	47

1979	41	9	1	0	7	59	43	10	1	0	18	57	78	25	2	0	4	22
1980	39	11	1	0	5	61	43	9	1	1	16	57	82	28	2	0	3	18
1981	42	12	2	0	12	58	48	21	4	2	17	52	44	13	1	2	14	56
1982	39	11	1	1	15	61	25	9	2	0	29	75	58	24	6	6	16	42
1983	48	19	6	0	15	52	45	14	1	1	11	55	65	25	2	1	10	35
1984	27	10	2	1	28	73	69	33	16	0	5	31	46	8	1	2	13	54
1985	68	25	3	0	3	32	31	8	1	1	23	69	48	9	2	1	8	52
1986	49	14	2	0	13	51	33	5	1	1	19	67	61	17	3	4	12	39
1987	66	22	4	0	4	34	39	6	1	2	15	61	62	26	3	1	8	38
1988	56	16	1	0	2	44	23	6	1	3	29	77	71	25	0	1	7	29
1989	48	19	4	0	11	52	70	28	7	1	6	30	43	5	1	3	17	57
1990	56	19	2	0	6	44	50	9	1	0	8	50	49	11	1	2	10	51
1991	33	4	0	2	10	67	60	24	5	0	3	40	73	26	3	1	4	27
1992	52	14	3	1	7	48	55	17	5	0	4	45	52	14	1	5	18	48
1993	59	18	2	1	4	41	45	9	1	0	16	55	48	17	2	2	21	52
1994	59	18	2	0	4	41	27	6	2	1	25	73	41	11	0	3	17	59
1995	34	10	3	3	19	66	58	23	3	1	15	42	48	8	1	8	20	52
1996	26	7	2	2	22	74	72	30	4	0	4	28	56	10	1	2	14	44
1997	35	3	0	1	18	65	46	16	3	2	12	54	18	4	2	9	50	82
1998	33	7	2	3	17	67	39	12	3	1	19	61	32	11	1	7	25	68
1999	24	4	1	1	35	76	59	23	12	1	7	41	51	13	2	7	16	49
2000	63	16	4	0	5	37	60	18	2	0	9	40	37	6	0	4	22	63
2001	67	28	7	0	5	33	38	15	1	1	22	62	42	17	1	3	15	58
2002	17	2	0	5	31	83	57	21	4	1	5	43	32	6	0	12	30	68
2003	58	28	4	1	8	42	35	5	1	0	20	65	52	9	1	6	18	48
2004	33	3	1	0	17	67	43	12	2	1	25	57	30	7	1	12	35	70
2005	61	20	1	0	4	39	47	15	2	0	12	53	35	4	0	2	19	65
2006	49	11	2	0	8	51	72	32	7	0	5	28	59	15	0	1	10	41
2007	28	5	1	0	23	72	68	24	5	1	5	32	28	3	1	9	28	72
2008	46	21	5	3	19	54	69	27	6	0	8	31	42	9	1	4	23	58
2009	23	5	0	1	32	77	73	23	9	0	4	27	29	4	0	3	25	71
2010	75	40	11	0	9	25	41	10	1	1	21	59	73	19	1	1	7	27

713

714

715

716

717

718

719

720

721

722

723

724

725

726

727 **Table 3.** The same as Table 2, but only for the years with a positive (negative) SCD

728 anomaly and only for the three major stable snow regions: Northeast China (78

729 stations), North Xinjiang (21 stations) and the Tibetan Plateau (63 stations).

730

Year	Northeast China						North Xinjiang						Tibetan Plateau					
	P	1SD	2SD	-2SD	-1SD	N	P	1SD	2SD	-2SD	-1SD	N	P	1SD	2SD	-2SD	-1SD	N
1957	98	20	54	0	0	2	20	0	0	30	0	80	77	12	42	4	0	23
1959	1	0	0	58	14	99	89	0	44	0	0	11	45	3	15	5	0	55
1960	42	1	15	24	0	58	100	26	58	0	0	0	22	0	0	29	2	78
1963	13	0	0	35	5	87	24	0	0	19	5	76	22	0	0	27	0	78
1965	68	1	23	13	1	32	24	0	0	38	0	76	13	0	4	42	4	87
1967	20	0	0	43	13	80	75	0	20	10	0	25	26	0	7	14	0	74
1969	23	0	3	26	14	77	75	0	30	5	0	25	3	0	0	47	5	97
1973	90	4	55	0	0	10	38	0	0	5	10	62	34	2	10	20	0	66
1974	53	0	17	18	3	47	5	0	0	33	19	95	40	0	3	11	2	60
1977	74	5	26	5	0	26	95	0	71	5	0	5	40	6	17	6	0	60
1980	62	1	16	8	0	38	95	5	57	0	0	5	43	2	10	3	0	57
1983	63	3	19	3	0	37	24	0	0	24	0	76	95	24	38	0	0	5
1988	71	0	23	3	0	29	100	10	62	0	0	0	51	5	16	2	0	49
1990	39	0	0	13	1	61	33	0	5	19	0	67	81	3	38	0	0	19
1994	95	1	26	0	0	5	95	0	48	0	0	5	44	2	11	10	0	56
1995	32	0	1	13	4	68	10	0	0	29	19	90	76	10	31	0	0	24
1998	5	0	0	49	13	95	62	0	5	5	10	38	77	11	24	2	0	23
2002	4	0	0	43	21	96	24	0	0	19	5	76	20	0	2	13	0	80
2008	6	0	0	38	12	94	5	0	0	48	5	95	61	2	7	11	2	39
2010	92	17	50	3	0	8	100	10	55	0	0	0	14	0	5	49	2	86

731

732

733

734

735

736

737

738

739

740

741

742

743

744

745

746 **Table 4.** Number of stations with SCD, SCOD, and SCED trends, number of stations

747 with relationships of SCD, SCOD, and SCED, respectively, with TBZD, number of

748 stations with relationship between SCD and MAT, and number of stations with

749 relationship between SCD and AO (352 stations in total). All of them have two

750 significance levels, the 90% and 95%.

751

		SCD			SCOD			SCED		
		95%	90%	I*	95%	90%	I*	95%	90%	I*
Trend	Positive	18	35	136	93	136	124	1	2	43
	Negative	38	54	127	13	23	69	92	138	169
TBZD	Positive	156	193	137	0	2	63	85	115	203
	Negative	0	0	22	64	93	194	0	2	32
MAT	Positive	0	2	30						
	Negative	129	171	149						
AO	Positive	35	87	77						
	Negative	33	82	106						

752 (Note: I* for insignificant trends or relations)

753

754

755

756

757

758

759

760

761

762

763

764 **Figure Captions**

765 **Figure 1.** Locations of weather stations and major basins, mountains and plains
766 mentioned in the paper, overlying the digital elevation model for China.

767 **Figure 2.** Percentage of weather stations with different measurement lengths.

768 **Figure 3.** Annual mean snow cover days (SCDs) from 1980/81 to 2009/10 (a), and their
769 coefficients of variation (CV) (b).

770 **Figure 4.** Seasonal variation of SCDs; the number in the centre denotes annual mean
771 SCDs, the blue colour in the circle the SCDs for winter season, the yellow colour for
772 spring, and the red colour for autumn.

773 **Figure 5.** SCD anomalies in 1957 (a), 2002 (b) and 2008 (c), anomaly of snow cover
774 onset date (SCOD) in 2006 (d), and anomalies of snow cover end date (SCED) in
775 1957 (e) and 1997 (f).

776 **Figure 6.** Trends of annual mean SCDs (a), SCOD (b), and SCED (c) from the 352
777 stations of more than ten annual mean SCDs with Mann–Kendall test, and
778 relationships among the SCD and day with temperature below 0°C (TBZD) (d), mean
779 air temperature (MAT) (e), and Arctic Oscillation (AO) index (f).

780 **Figure 7.** SCD variations at Kuandian (40°43' N, 124°47'E, 260.1 m) (a), Hongliuhe
781 (41°32' N, 94°40'E, 1573.8 m) (b), Gangcha (37°20' N, 100°08'E, 3301.5 m) (c) and
782 Shiqu (32°59' N, 98°06'E, 4533.0 m) (d), SCOD at Pingliang (35°33' N, 106°40'E,
783 1412.0 m) (e) and Weichang (41°56' N, 117°45'E, 842.8 m) (f), and SCED at Jixi

784 (45°18' N, 130°56'E, 280.8 m) (g) and Maerkang (31°54' N, 102°54'E, 2664.4 m) (h).

785 (The unit on the Y-axis in the figures e, f, g, h denotes the Julian day using 1st

786 September as reference).

787 **Figure 8.** Spatial distribution of SCOD (a) and SCED (b) based on the stations with an

788 average of more than ten SCDs.

789 **Figure 9.** SCD relationships with TBZD at Chengshantou (37°24' N, 122°41'E, 47.7 m)

790 (a), MAT at Baicheng (41°47' N, 81°54'E, 1229.2 m) (b), and AO index at Huajialing

791 (35°23' N, 105°00'E, 2450.6 m) (c) and Tonghua (41°41' N, 125°54'E, 402.9 m) (d).

792

793

794

795

796

797

798

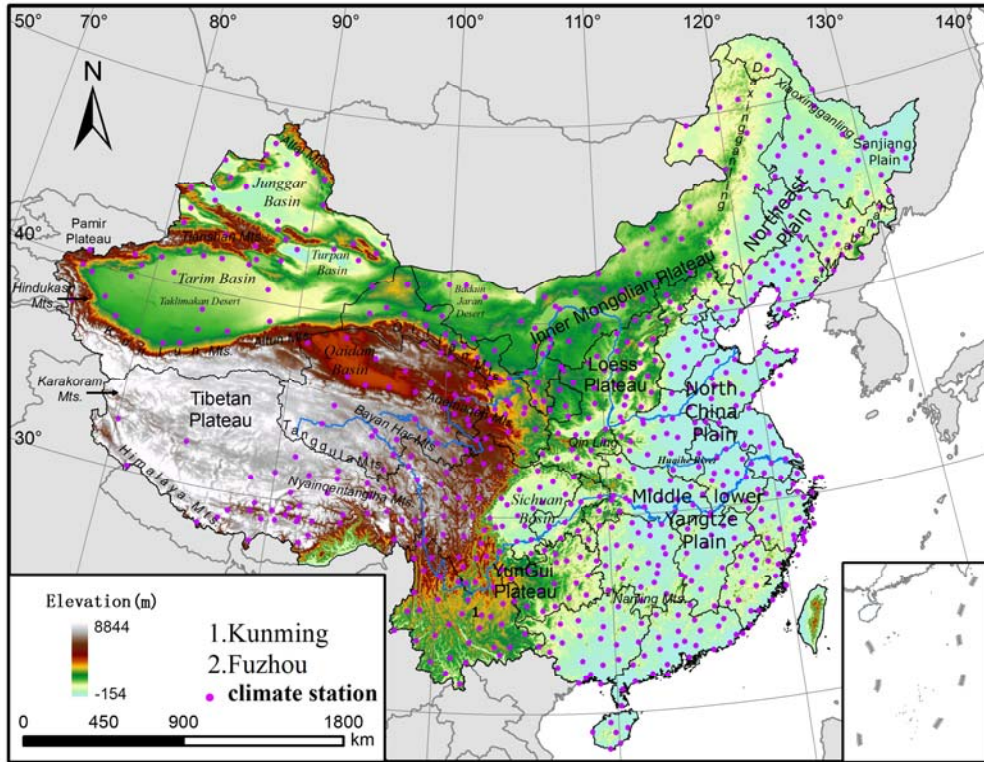
799

800

801

802

803

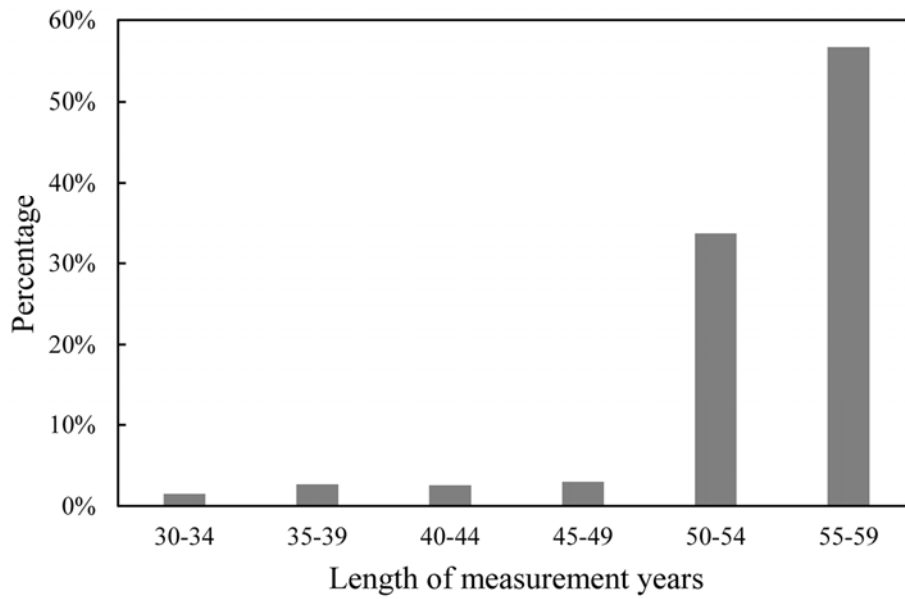


804

805

Figure 1

806

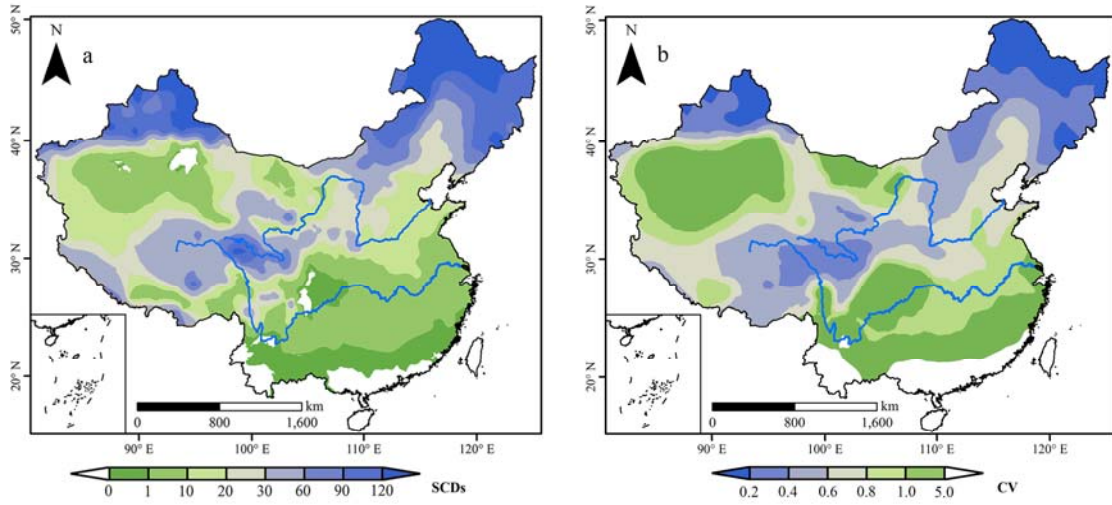


807

808

Figure 2

809

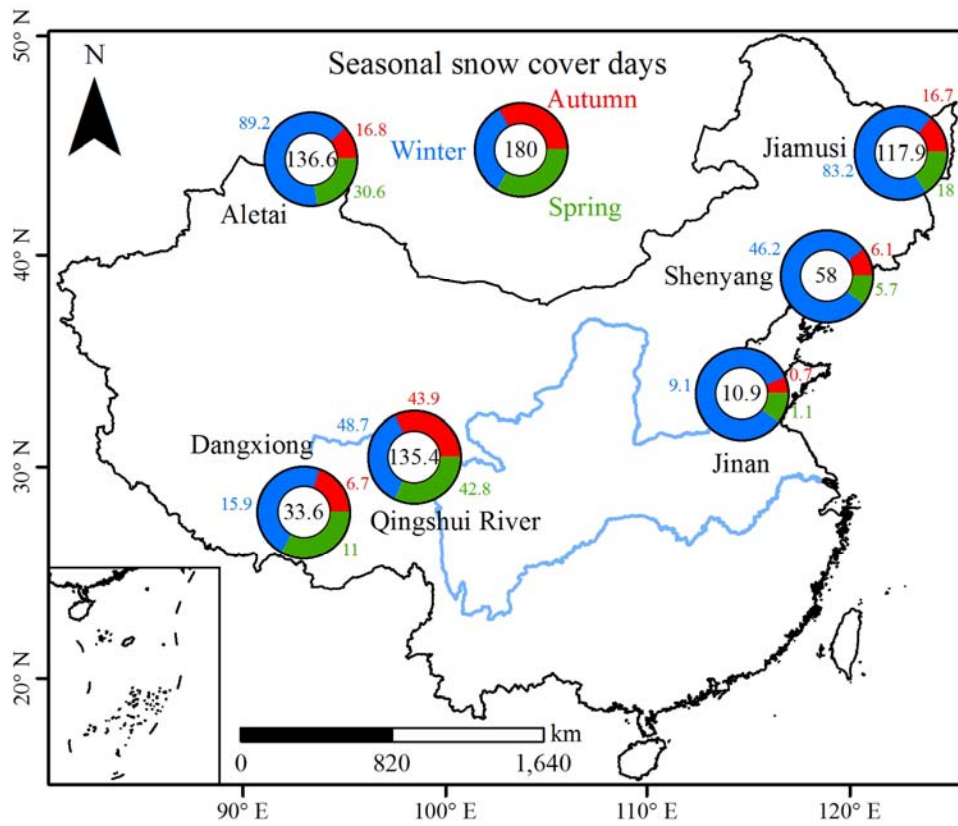


810

811

Figure 3

812

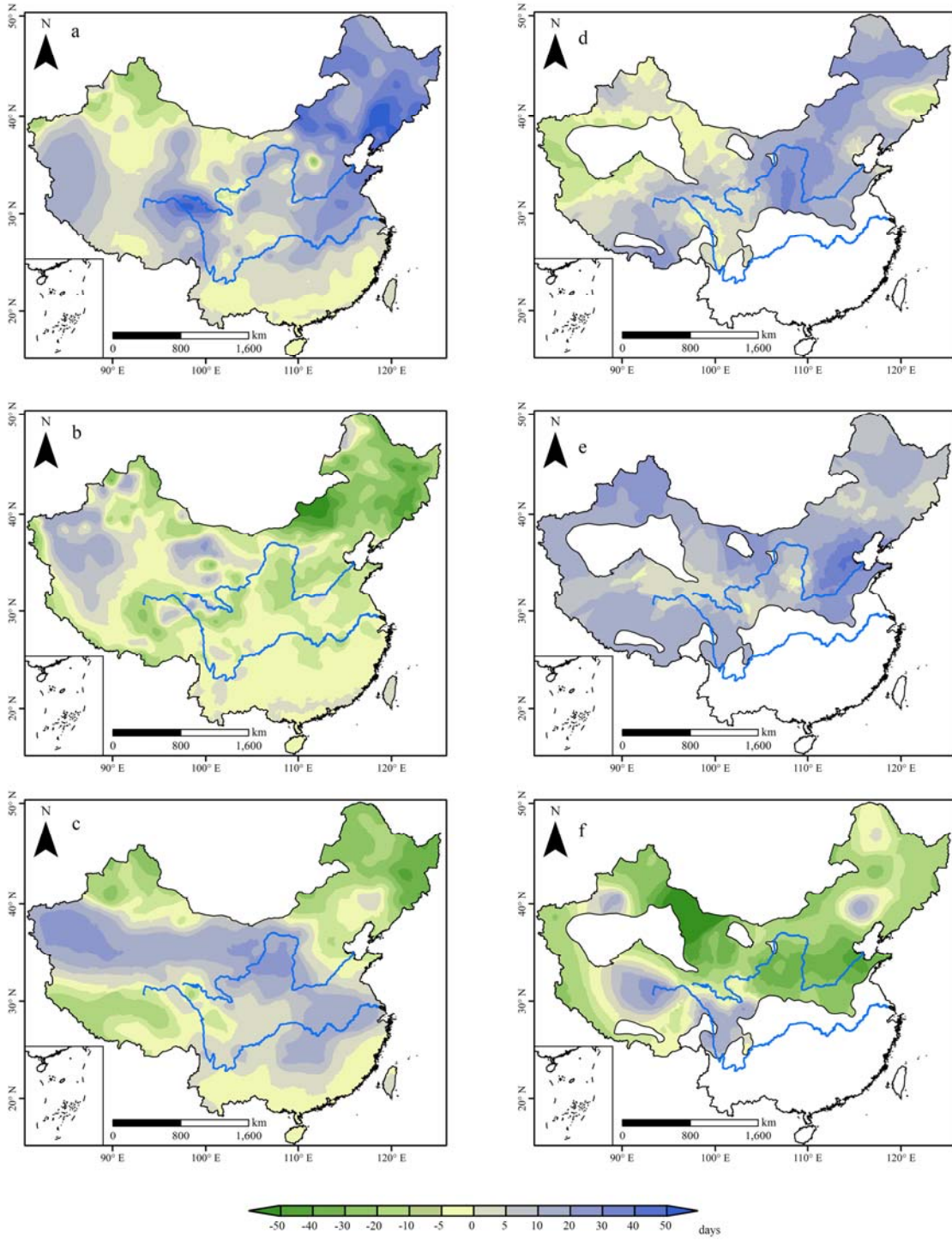


813

814

Figure 4

815

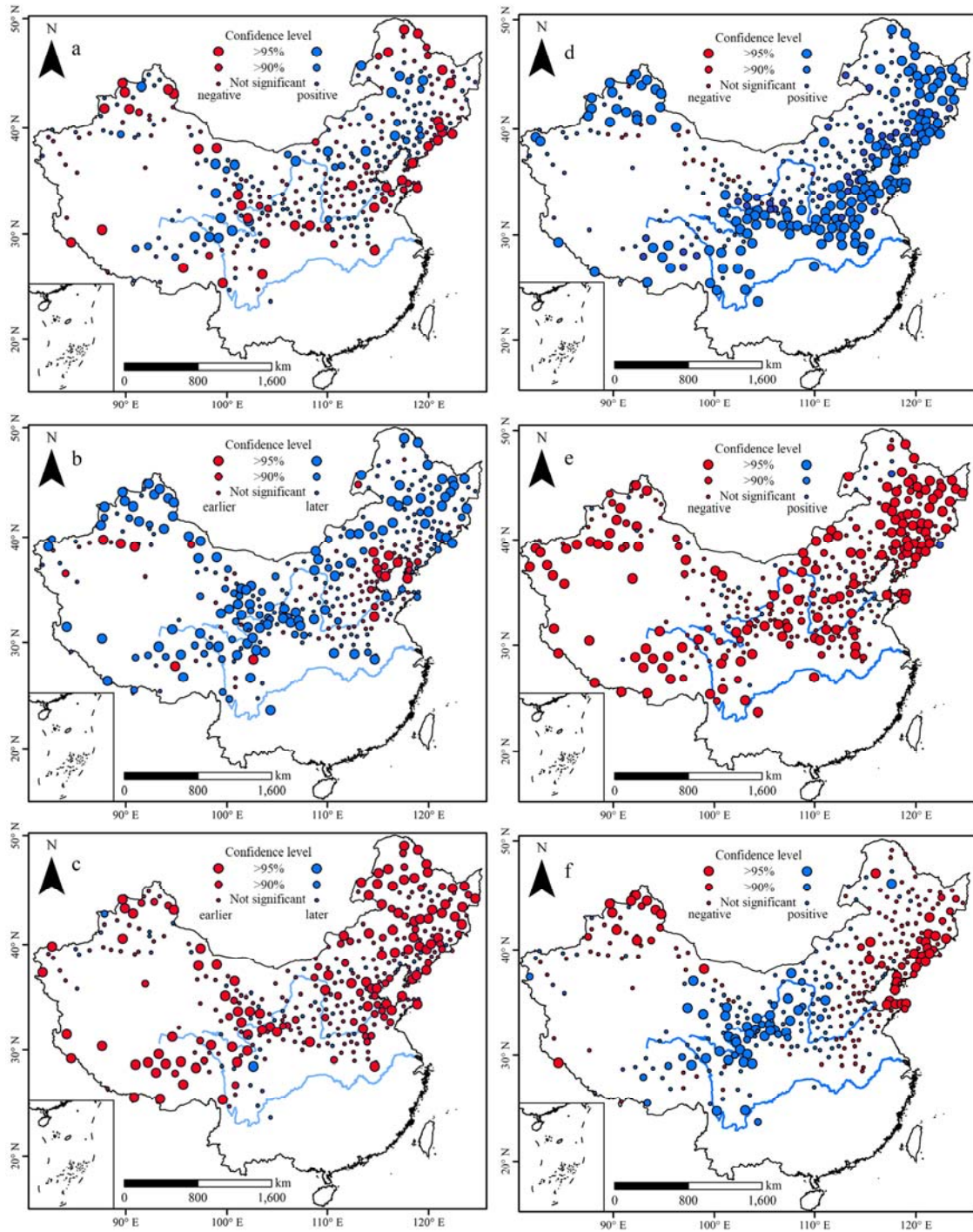


816

817

818

Figure 5



820

821

Figure 6

822

823

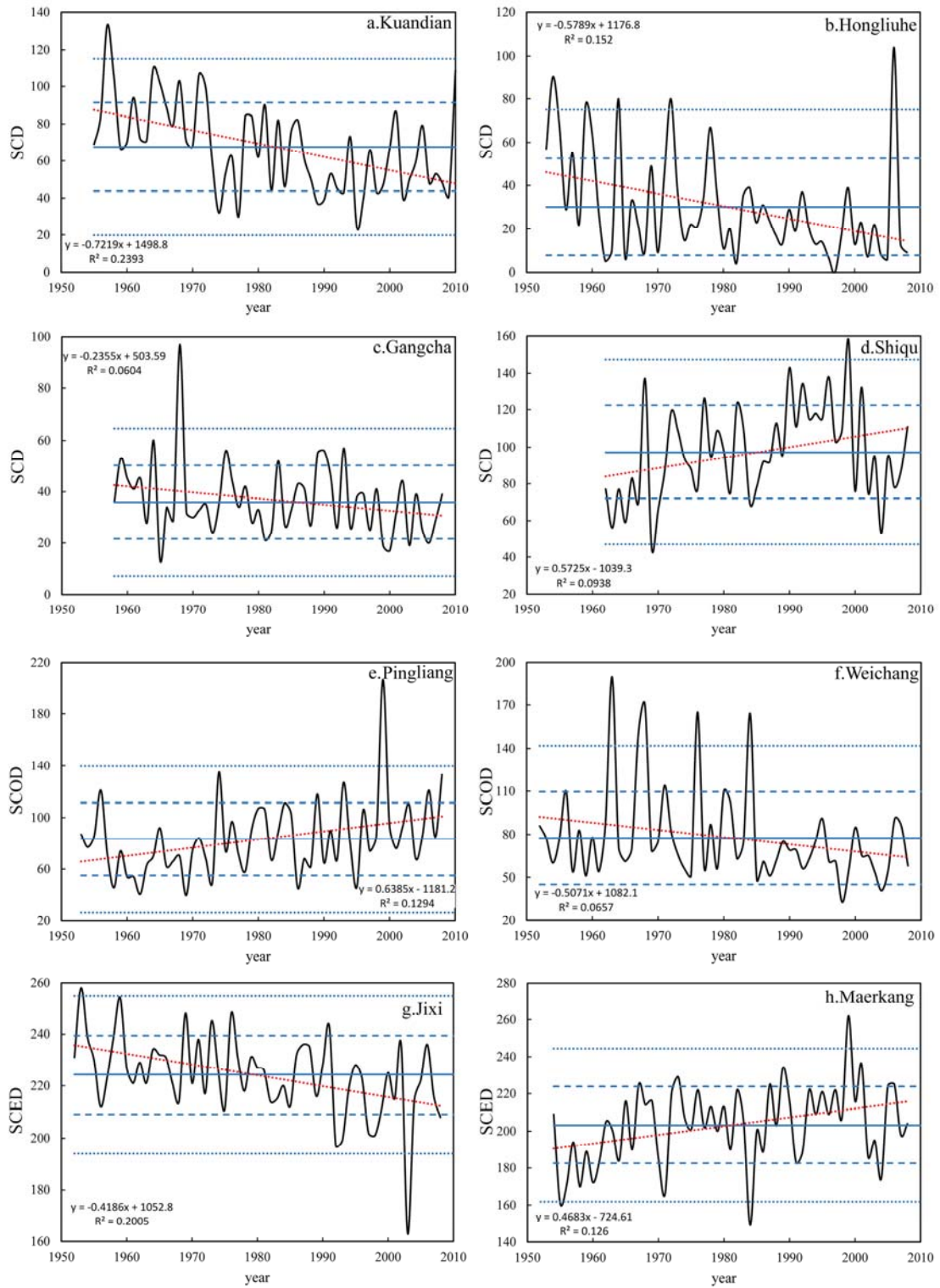
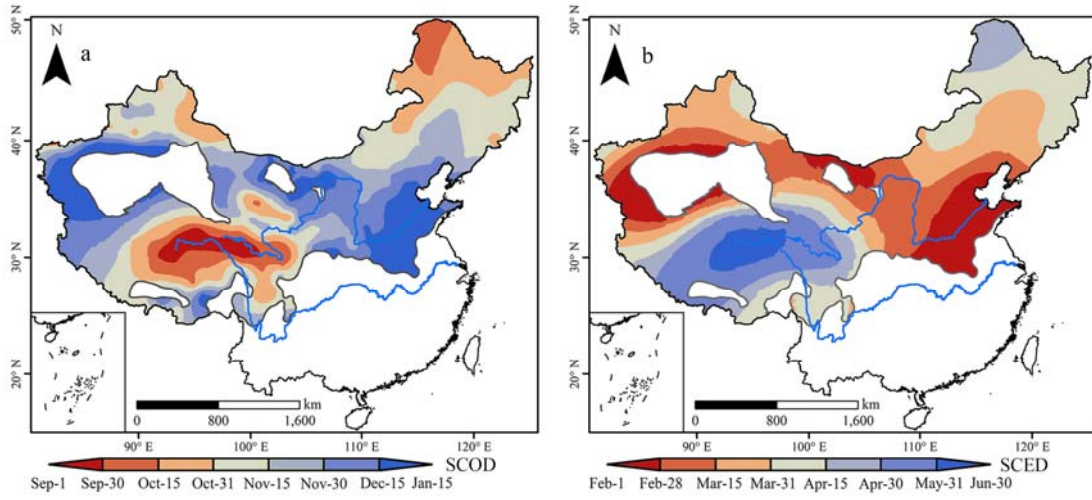


Figure 7

828

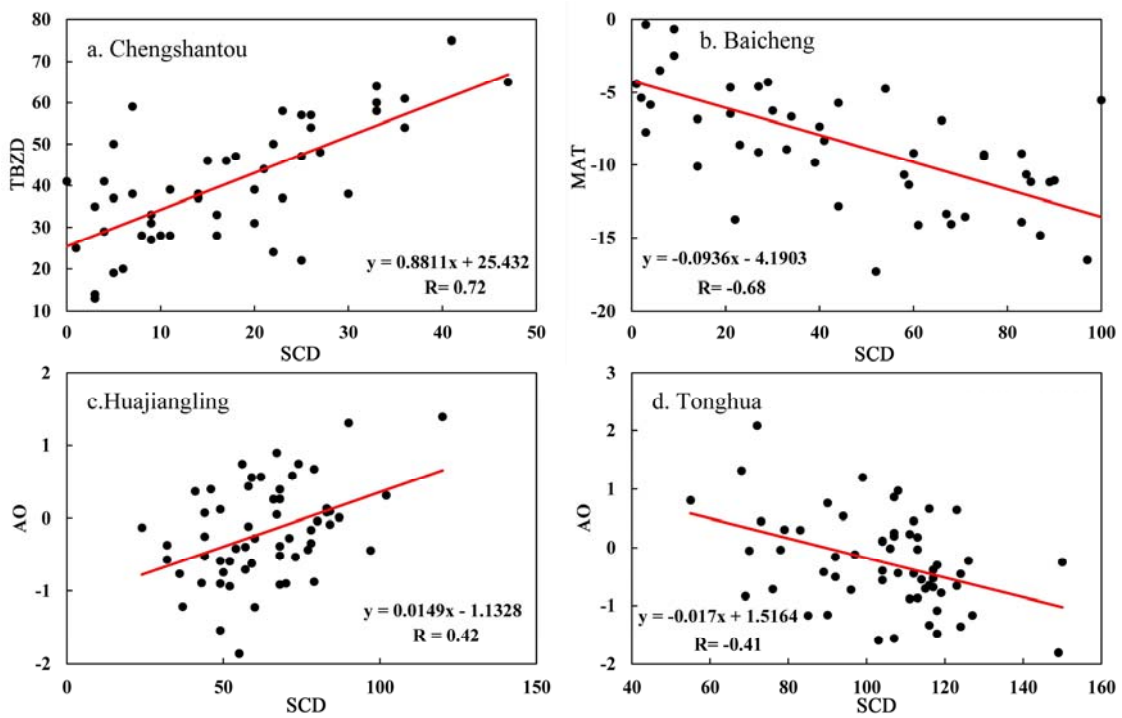


829

830

Figure 8

831



832

833

Figure 9

834